Similarity law for the tilt angle of dendrites in directional solidification of non-axially-oriented crystals

Silvère Akamatsu and Thomas Ihle*
Groupe de Physique des Solides, Universités Denis Diderot (Paris VII) et Pierre et Marie Curie (Paris VI), Tour 23, 2 place Jussieu, 75251 Paris Cedex 05, France
(Received 1 May 1997)

We report on an experimental and numerical study of tilted dendrites observed in thin-film directional solidification of a CBr_4–8 mol % C_2Cl_6 alloy for an arbitrary orientation of the crystal with respect to the plane of the sample and the pulling direction. The drift velocity V_d, or, equivalently, the tilt angle α (defined as $\tan\alpha = V_d/V$, where V is the pulling velocity) of the dendrites is an increasing function of V and the dendritic spacing λ. We show that α scales like the Péclet number $P = \lambda V/D$ (D is diffusion coefficient in the liquid). In the limit of large P values ($P > 7$), α tends to a constant, crystallographically determined value. We show that the α versus P master curve is insensitive to the temperature gradient as long as V is not too close to the cellular-threshold velocity. The tilt dynamics of dendrites in directional solidification is thus essentially determined by the interactions between neighboring dendrites within the approximately periodic pattern. We also show that the shape of the master curve only slightly depends on the value of the interfacial anisotropy, as long as it is not too small. [S1063-651X(97)14310-0]

PACS number(s): 68.70.+w, 81.10.Aj, 64.70.Dv, 81.30.Fb

I. INTRODUCTION

The most frequently encountered growth morphology of nonfaceted crystals (diffusion-controlled growth) is the dendrite [1–4]. In free growth, i.e., the growth of a crystal from a unique solid germ in a uniformly cooled melt, dendrites grow isolated from each other. The dendritic shape is then a ''needle crystal'' with a parabolic tip affected on its sides by a secondary branching. At given undercooling, the dendrite-tip radius of curvature ρ and the tip velocity are uniquely selected by the anisotropy of the surface stiffness τ [1] or the kinetic coefficient β [2]. The dendrites moreover grow parallel to symmetry axes of the crystal corresponding to the directions of the minimums of τ or β. For cubic crystals [3], these directions generally are $\langle 100\rangle$ axes. In directional solidification [4], the melt is solidified at constant velocity V in an externally imposed, unidirectional temperature gradient. In thin samples, the growth pattern is then essentially periodic. At sufficiently high values of V above the cellular-threshold velocity V_c [5], one observes regular arrays of dendrites. Within such patterns, each dendrite interacts with its neighbors via the diffusion field in the liquid (finite-size effects), the strength of this interaction being obviously a decreasing function of the inter-dendritic spacing λ.

In thin samples, the growth pattern strongly depends on the orientation of the crystal with respect to the solidification setup. The reason for this is that the system practically behaves in a two-dimensional (2D) way, as shown in Ref. [4]. This means that, in spite of the fact that the solid-liquid interface necessarily forms a meniscus, it can be considered that the normal of the solid-liquid interface remains parallel to the plane of the sample. The pattern is only sensitive to the strength and form of the anisotropy of the crystal within this plane [4]. In directional solidification, the orientation of the crystal must be specified not only with respect to the sample plane, but also with respect to the axis of the temperature gradient, which is also the imposed average growth (or pulling) axis. Let z be the pulling axis and x the axis normal to z and parallel to the plane of the sample. Let c be the direction of the minimum of τ or β within the sample plane and α_0 the angle between z and c. Except for axially oriented crystals—i.e., the particular case where a $\langle 100\rangle$ axis of the (cubic) crystal, or its projection onto the sample plane, is parallel to z—α_0 is nonzero. The dendritic pattern then drifts at a constant velocity V_d along the front (Fig. 1) [4,6–7]. The tilt angle α of the dendrites, defined by $\tan\alpha = V_d/V$, is of same sign as but smaller (in absolute value) than α_0. Contrary to free-growth dendrites, directional-solidification dendrites generally grow along a direction that is not that of the minimum of τ or β.

In this paper, we focus on the quantitative dependence of α on the various relevant parameters, namely, the temperature gradient G, the pulling velocity V, the dendritic spacing λ, and the orientation of the crystal. To this purpose, we performed directional solidification experiments of CBr_4-C_2Cl_6 alloys at a fixed concentration $C_\infty = 8$ mol %. We also carried out numerical calculations (resolution of the equations of the minimal model of diffusion-controlled growth in two dimensions in a channel with periodic boundary conditions) with the help of a dynamic code adapted from that used in Ref. [4]. *A priori*, the difference between α and α_0 can be expected to depend on both the interactions between neighboring dendrites and the strength of the temperature gradient. We indeed observe that the tilt angle of the dendrites is an increasing function of V (as already shown

*Present address: Laboratoire de Spectrométrie Physique, Université Joseph Fourier (Grenoble I), Boîte Postale 87, 38402 St. Martin d'Hères Cedex, France.

 © 1997 The American Physical Society

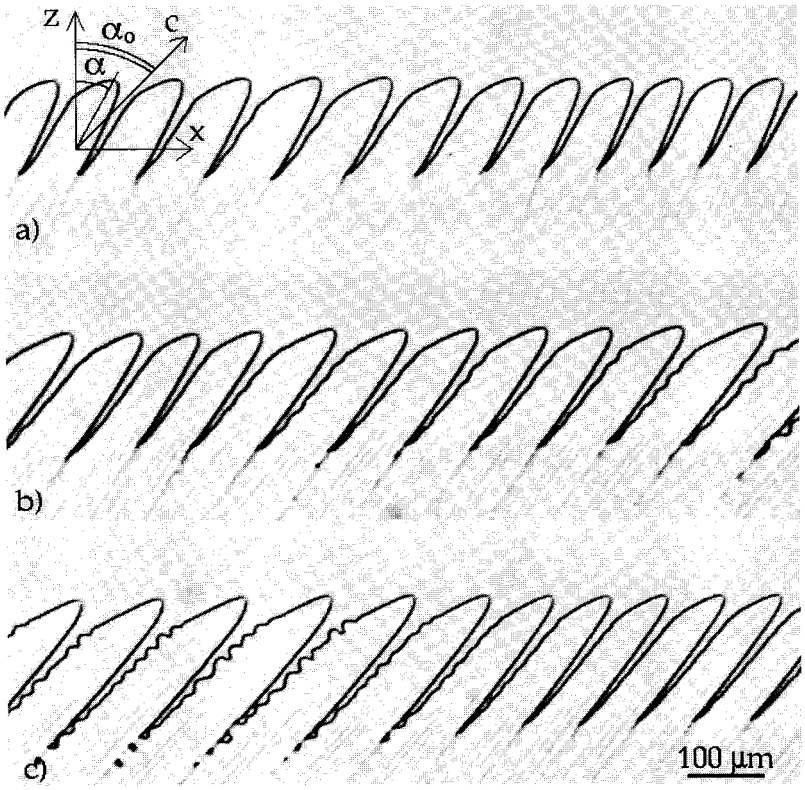

FIG. 1. Tilted-dendrite patterns in directional solidification of a CBr_4–8 mol % C_2Cl_6 alloy for three different pulling velocities: (a) 9.94 μm s^{-1}; (b) 13.5 μm s^{-1}; (c) 23.9 μm s^{-1}. z axis: pulling axis; α: tilt angle of the dendrite; α_0: angle between the z axis and the c axis (see text).

experimentally by Trivedi *et al.* [6] and Oswald *et al.* [7] in the pivalic acid–ethanol system) and also of λ. The dependence of α on λ, which has never been quantitatively demonstrated before, is not a surprise in view of the preceding remarks. More unexpectedly, we find that, for pulling velocities sufficiently higher than V_c, α is practically a function of only one variable, namely, the spacing Péclet number, defined as $P=\lambda/l_d$, where $l_d=D/V$ is the diffusion length (D is the diffusion coefficient of the solute in the liquid). This means that the tilt angle of dendrites is determined by finite-size effects, independently of the value of G. These results are found both experimentally and numerically. In addition, numerical calculations show that, at given P, α scales almost linearly with α_0 for α_0 values up to $\approx 25°$. We also investigated numerically the dependence of α on the strength of the interfacial anisotropy.

II. EXPERIMENTAL AND NUMERICAL METHODS

For the directional solidification experiments, the concentration of C_2Cl_6 in the CBr_4-C_2Cl_6 alloy was fixed to 8 mol %. The alloy was made with zone-refined and outgassed materials. The temperature gradient was set to $G=110 \pm 10$ K cm^{-1}. The calculated value of the cellular-threshold velocity V_{cs} in the constitutional supercooling approximation is ≈ 2.5 μm s^{-1}. We recall that $V_{cs}=DG/\Delta T_0$, where $\Delta T_0 = m(K^{-1}-1)C_\infty$ is the thermal gap, m the slope of the liquidus, and K the partition coefficient (see Table I) [5]. Experimentally, we measured the actual value of the cellular threshold $V_c^{\text{expt}}=2.2\pm 0.4$ μm s^{-1}. The fact that V_c^{expt} is smaller than V_{cs} stems from the presence of a small amount of residual impurities in the alloy [8,9]. Two facts evidence that residual impurities do not markedly perturb our experiments. First, the initial solute-redistribution transient [10] is well completed within about 5 times the diffusion time $\delta = D/V^2$, and the long-lasting recoil of the front previously recorded in the most contaminated samples was not observed. Second, no gas bubbles were observed to preexist in the liquid or nucleate in the course of solidification runs (low residual-gas concentration).

We used thin (≈ 12 μm thick), ''funnel-shaped'' samples [4] in order to select large (≈ 8 mm wide) single crystals. However, the selection procedure of the single crystal is performed without any quantitative knowledge of the anisotropy and α_0. X-ray analysis for the determination of the crystal orientation cannot be used because a solid-solid transition undergone by the CBr_4-C_2Cl_6 alloy at about 43 °C induces a polygonization of the initial single crystal. We did not use the ''faceted-bubble'' method explained in Ref. [4] in order to avoid plastic deformations of the crystal when a bubble is being entrapped by the solid [11].

Each solidification run was performed by increasing V through discrete velocity jumps within a range of $4-31$ μm s^{-1}, i.e., $1.4V_{cs}$ to $11V_{cs}$. After each V jump, we waited a time much longer than δ (or D/V_1V_2 for a velocity jump from V_1 to V_2) [10]. It can be seen in Fig. 1, which shows three tilted-dendrite fronts observed in the same single crystal at three different velocities, that λ is not uniform

TABLE I. Physical constants of the CBr_4-C_2Cl_6 alloy. The values of m, K, D, and d_0 (symbols: see text) are known within ±20% [9]. The melting temperature T_m of pure CBr_4 is known ±0.3 °C. The determination of β_0 [14] is explained in Sec. II.

T_m (°C)	$\lvert m\rvert$ (K/mol %)	K	D (cm^2 s^{-1})	d_0 (μm)	β_0 (K s μm^{-1})
92.5	0.8	0.75	5×10^{-6}	0.054	4.46×10^{-3}

along a given front. These smooth λ modulations are observed to persist over very long times ($\gg\delta$) and, except when λ gradients are too steep, they travel rigidly with the pattern, which shows that λ is not selected and phase diffusion is ineffective. The λ modulations are thus history dependent and remain essentially unchanged since the initial instability of the front. This is true even when V jumps are applied, provided that the amplitude of the jumps remains moderate (i.e., such that no cell termination, or tip splitting, or tail instability occur; in practice, this is always fulfilled by increasing V by a factor less than 2). As a consequence, the mean value of the dendritic spacing and the width of the λ distribution does not change much when V is varied. There are, nevertheless, some changes that are due to the fact that the drifting pattern is continually generated at a source point (the edge of the sample opposite to the drift direction, in the case of Fig. 1 the left-hand edge) and that the value of λ delivered by this source depends on V. This means that the patterns that we have studied were never perfectly steady. We took care to measure α only in quasisteady situations. α measurements were done by recording spatiotemporal diagrams over long times (more than ten times δ) from images of about a third (2.5 mm) of the whole front (this corresponds to about 25–40 cells or dendrites, according to the mean value of λ).

Numerical calculations were performed in two dimensions in a channel with periodic boundary conditions [4], as mentioned above. We included a linear interfacial kinetics into the Gibbs-Thomson equation, which reads

$$u_i = 1 - d\kappa - \frac{\beta v}{\Delta T_0}, \tag{1}$$

where $u_i = (C - C_\infty)/\Delta C_0$ is the reduced concentration at the interface ($\Delta C_0 = \Delta T_0/m$ is the concentration gap), κ the curvature of the interface, d the capillary length, and v the velocity of the interface. Both d and β are assumed to depend on the orientation of the crystal. The inclusion of an anisotropic kinetic coefficient was motivated by our previous observation [4] that the tip region of the dendrites in CBr_4-C_2Cl_6 alloys at $V \gg V_c$ exhibits a pronounced angular shape and a weak-amplitude sidebranching. A detailed numerical study of the shape of the dendrites as a function of β and its anisotropy, which will be reported elsewhere [12], led us to the conclusion that, as suggested by Classen *et al.* [13], the kinetic anisotropy even dominates the capillary one in the dendritic-selection mechanism in our system. We took the following formulas for d and β:

$$d(\theta) = d_1[1 - \varepsilon_c \cos 4(\theta - \alpha_0)], \tag{2}$$

$$\beta(\theta) = \beta_1[1 - \varepsilon_k \cos 4(\theta - \alpha_0)], \tag{3}$$

These functional forms are appropriate for crystal orientations such that a [100] axis nearly lies within the sample plane. In this case, the c axis practically coincides with the projection of the [100] axis onto the sample plane. The coefficients β_1, d_1, ε_k, and ε_c (but not α_0) depend on the off-plane misorientation of the [100] axis [4]. Quantitatively, the dependence of β_1 and d_1 on the crystal orientation is negligible. We took them equal to their values β_0 and d_0 averaged over all orientations. On the other hand, for symmetry reasons, ε_k and ε_c have the same, strong dependence on the crystal orientation. They are maximum when a ⟨100⟩ axis lies in the plane of the sample, and decrease as the off-plane misorientation of this axis increases. The value $\beta_0 = 4.46 \times 10^{-3}$ K s μm^{-1} [14], and the values $\varepsilon_k = 0.12$ and $\varepsilon_c = 0.06$ in a (100) plane were determined so as to fit the shape of axial dendrites observed for a crystal orientation such that a [100] axis is nearly parallel to the z axis [12]. The value of the other physical constants used in the calculations, which have been independently determined in a previous study [8], are reported in Table I. In the present study, the concentration was fixed to 8 mol % and the temperature gradient to $G = 80$ K cm^{-1} ($V_{cs} = 1.85$ μm s^{-1}). Most of our calculations have been performed for $\alpha_0 = 30°$. In Fig. 2 is shown a simulation of an array of four tilted dendrites calculated with $\alpha_0 = 45°$ and $\lambda = 155.2$ μm at $V = 6V_{cs}$ ($P = 3.44$ and $\alpha = 35°$). The calculation is made in a channel of relatively large width $w = 4\lambda$ to ensure that the extended, stationary pattern is intrinsically stable. For this α_0 value, unstable patterns are observed in the absence of kinetic anisotropy. It can be seen in Fig. 2 that the successive images of the interdendritic liquid grooves overlap. This entails that the angle of the grooves with the z axis is slightly higher than α. Finally, experiments as well as calculations show that the shape of tilted dendrites is asymmetric with respect to the tilt axis. The point of maximum curvature is neither the point of lower undercooling nor the point at which the normal to the interface is parallel to the tilt axis. The detailed study of the shape of tilted dendrites is in progress and will be reported elsewhere.

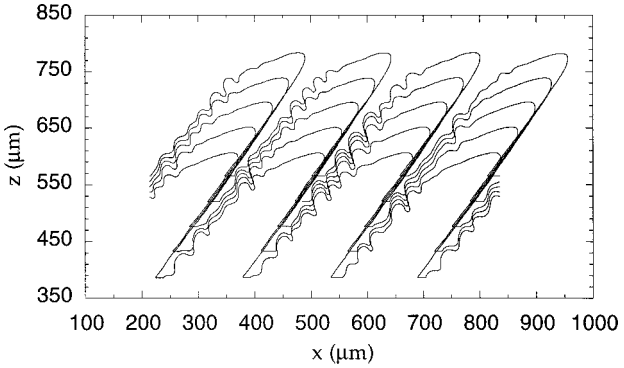

FIG. 2. Tilted dendrites obtained in a numerical calculation in a channel with periodic boundary conditions of the directional solidification of a CBr_4–8 mol % C_2Cl_6 alloy ($\alpha_0 = 45°$). $V = 6V_{cs}$; $\lambda = 155.2$ μm; $P = 3.44$ and $\alpha = 35°$; channel width: 4 λ.

III. RESULTS

The values of α measured during the same three experimental runs as in Fig. 1 are plotted in Fig. 3 as a function of λ. The reading errors are much smaller than the scatter of the data points, which is mainly due to the fact that the patterns are not strictly stationary (see above). Figure 3 primarily shows that, at fixed V, α markedly increases when λ increases. In addition, it confirms that, at fixed λ, α increases when V increases [5,6]. Figure 4 shows the dependence of α on the spacing Péclet number P for two different crystals (crystal 1 is the same crystal as in Figs. 1 and 3). For each

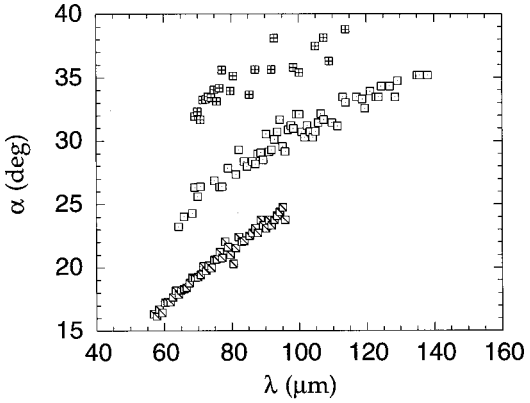

FIG. 3. α as a function of λ measured at $V=9.94\ \mu\mathrm{m\ s^{-1}}$ (⧅), $V=13.5\ \mu\mathrm{m\ s^{-1}}$ (⊡), and $V=23.9\ \mu\mathrm{m\ s^{-1}}$ (⊞) in the same crystal as in Fig. 1.

crystal, the data points fall onto a single, well-defined curve. This similarity-law behavior is confirmed by the numerical calculations reported in Fig. 5 (see also Table II). We calculated three sets of data points for $\alpha_0=30°$ for three values of λ, namely, 55.9, 79.0, and 162.8 μm, which fall within the experimentally observed range. The value of V was varied between $1.7V_{cs}$ and $14V_{cs}$, so that P varied between 0.5 and 7. The three numerical sets of data coincide within numerical errors ($\pm 0.3°$) for P ranging from about 0.9 to 7. The slight discrepancy between the two points at $P=0.6$ will be commented on in the next section.

In our experiments, the value of α_0 is not known independently of the growth pattern. We thus cannot directly compare the numerical data to the experimental ones. However, our experimental and numerical results show that, at high P values, α tends towards a constant value, which depends on the crystal orientation. The calculations moreover show that this limit value is equal (or, at least, extremely close) to α_0. From Fig. 4, it can be seen that this limit value is roughly equal to 40° for crystal 1 and 32° for crystal 2 (the experimental error being about $\pm 2°$). This yields thus a

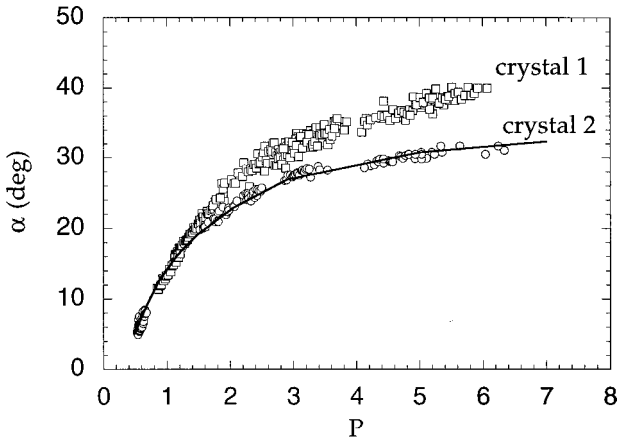

FIG. 4. α as a function of P (see text) measured experimentally for two crystals of different orientations. Crystal 1 (□) corresponds to the same crystal as in Figs. 1 and 3. The thin line is a guide for the eyes and corresponds to numerical points calculated for $\alpha_0=30°$ (see Fig. 5 and Table II) rescaled so that it fits the experimental points of crystal 2 (○).

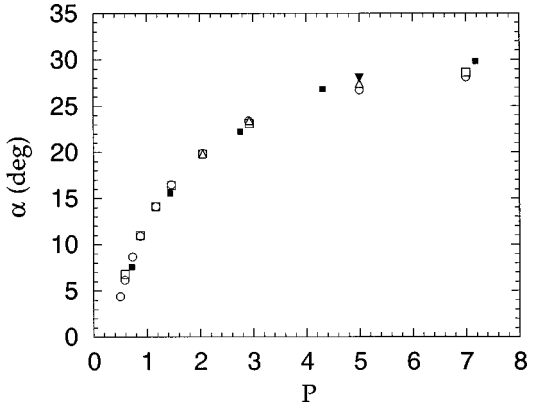

FIG. 5. α as a function of P calculated numerically ($\alpha_0=30°$) for $\lambda=55.9\ \mu$m (○), $\lambda=79\ \mu$m (□), and $\lambda=162.8\ \mu$m (△) at various velocities. The point calculated at $P=5$ and for $\alpha_0=17°$ (▼) and the numerical results obtained by Okada and Saito [16] (■) also for $\alpha_0=17°$ are rescaled by a factor 1.76 (see text).

method for estimating α_0, which simply consists of extrapolating the measured values of α to high values of P. One has, however, to take care of the fact that the α versus P curves only saturate for relatively high P values. In the case of the curve calculated for $\alpha_0=30°$ (Fig. 5), the difference between α and α_0 is $\approx 6°$ at $P=5$, and still $\approx 2°$ at $P=7$. On the other hand, we calculated that, for $\alpha_0=17°$, $\alpha=15.9\pm 2°$ at $P=5$, which seems to indicate that the α versus P curve approaches its asymptotic value more rapidly as α_0 is decreased.

This last result signals that the shape of the α versus P curve varies according to the value of α_0. On the one hand, we show in Fig. 4 that it is possible to fit the whole α versus P curve calculated for $\alpha_0=30°$, multiplied by a factor ≈ 1.15, to the experimental data of crystal 2, which, as estimated above, corresponds to a value of α_0, which is not very different from 30°. On the other hand, the same procedure applied to crystal 1 gave unsatisfactory results, indicating that the shape of the α versus P curve changes significantly from $\alpha_0\approx 30°$ to $\alpha_0=40°$. This can be understood by studying the dependence of α on α_0 at a fixed value of P. Figure 6 shows that, for $P=2.93$ and α_0 ranging between 0 and 47°

TABLE II. α as a function of P for different values of λ (numerical results) and $\alpha_0=30°$; see text for symbols.

	α (deg)			
P	$\lambda=55.9\ \mu$m	$\lambda=79.0\ \mu$m	$\lambda=95.6\ \mu$m	$\lambda=162.8\ \mu$m
0.49725		4.4		
0.585	6.8	6.2		
0.73125		8.7		
0.8775	11.0	10.9		
1.17	14.1	14.1		
1.4625	16.4	16.5		
2.0475	19.8	19.9		19.8
2.91		23.4		
2.925	23.1			23.4
5	26.7		27.2	27.4
7	28.1		28.6	

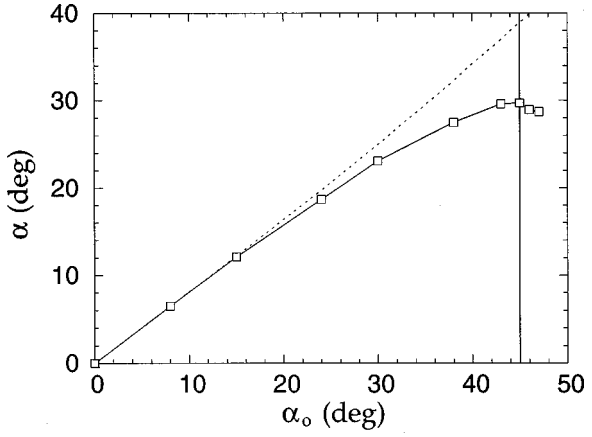

FIG. 6. α as a function of α_0 for $P=2.925$ ($\lambda=55.9\ \mu$m) (numerical results). The line joining the data points is only a guide for the eye. Dotted line: straight line passing through the first two data points.

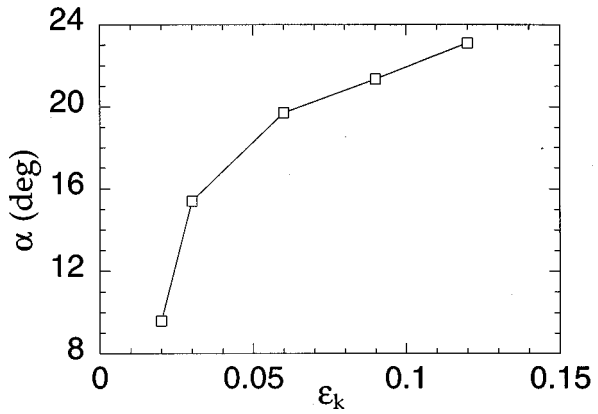

FIG. 7. Dependence of α on ε_k for $P=2.925$ and $\alpha_0=30°$ (numerical results). The ratio $\varepsilon_k/\varepsilon_c=2$ is kept constant. The line is only a guide for the eye.

(see also Table III), the dependence of α on α_0 is roughly linear for $0<\alpha_0\lesssim 25°$. Within this range of values of α_0, the α versus P curves corresponding to different values of α_0 can be rescaled so that they fit each other, the scaling factor being then exactly equal to $1/\alpha_0$. In other words, the α/α_0 versus P curve can be used as a master curve, and the knowledge of α for any value of P is sufficient to know α_0. For α_0 higher than 25° (as in the case of crystals 1 and 2), the variations of α with P and α_0 cease to obey this additional similarity law.

Finally, in the experiments, not only α_0, but also ε_k, varies from one crystal orientation to another. We studied numerically the sensitivity of α to ε_k ($\varepsilon_k/\varepsilon_c=2$ being kept constant) at a given P value of 2.925 and $\alpha_0=30°$ (Fig. 7; see also Table IV). It can be seen that α increases when ε_k increases, this dependence being particularly strong when ε_k is small ($\varepsilon_k<0.06$). However, it must be noted that, in this low-anisotropy range, calculations have shown that, as V and λ are increased, the pattern becomes sensitive to instabilities that are clearly a precursor of the formation of doublons and the ''seaweed pattern'' [4]. These instabilities were not observed during the solidification of crystals 1 and 2. Our experiments thus clearly correspond to the ''high''-anisotropy range ($0.06<\varepsilon_k$), within which the variations of α with ε_k are small. The direct comparison made in the preceding paragraph between the α versus P curves obtained experimentally and numerically, which assumed implicitly that a [100] axis nearly lies within the sample plane, is thus justified. From Fig. 7, one deduces that the above fitting procedure applied to crystal 2 delivers a value of α_0 ($1.15\times 30=34.5°$) is accurate within $\approx 15\%$, which remains of the same order of magnitude as the experimental uncertainty.

TABLE III. α as a function of α_0 (numerical results) for $P=2.93$ (see text).

α_0 (deg)	α (deg)
8	6.47
15	12.1
24	18.7
30	23.1
38	27.5
43	29.6
45	29.7
46	28.95
47	28.7

IV. DISCUSSION

The growth dynamics in directional solidification *a priori* depends on the relative values of the characteristic lengths l_d, [$l_t=\Delta T_0/G$ (thermal length)], d_0, and λ (a ''kinetic length'' $k_0=D\beta_0/\Delta T_0$ can also be defined from the kinetic coefficient β_0 [14]). Moreover, it generally suffices to consider three reduced parameters, constructed from these four characteristic lengths, and which are (i) the spacing Péclet number P, (ii) the parameter $\mu=l_t/l_d=V/V_{cs}$, and (iii) the parameter d_0/l_t (or, rather, k_0/l_t). As mentioned above, the first parameter (P) measures the interactions between neighboring dendrites via the diffusion field. Since, in the present study, C_∞ is fixed, the second parameter (μ) measures the influence of the temperature gradient. Contrary to l_t and l_d, the lengths d_0 and k_0 are not observable directly. Knowing that, except for very dilute alloys (which is not the case here), the ratios d_0/l_t and k_0/l_t are extremely small (in the range 10^{-4}–10^{-3}) is not sufficient to decide if these quantities are relevant or not for the determination of the tilt angle of the dendrites. However, as d_0 and k_0 set the scale for the tip radius ρ of the dendrites, it can be assumed that the influence of d_0/l_t and k_0/l_t can be neglected as long as the

TABLE IV. α as a function of ε_k (numerical results) for $P=2.93$ (see text). Note that $\varepsilon_k/\varepsilon_c=2$ is kept constant.

ε_k	α (deg)
0.02	9.6
0.03	15.4
0.06	19.7
0.09	21.35
0.12	23.1

ratio ρ/l_t is small, which is the case here.

Our results show that, in directional solidification, the deviation of the dendritic-growth axis from the preferred growth axis c, i.e., the difference between α and α_0, is only a function of P. This means that $\alpha-\alpha_0$ is insensitive to the value of G. We obtained additional evidence of this property by calculating α at a given value of $P=2.925$ ($\lambda=55.9\ \mu$m) for two values of G (40 and 160 K cm^{-1}) differing from each other by a factor 4. These calculations gave the same value of $\alpha=22.6°$ within numerical errors ($\pm 0.3°$). This also explains the quantitative agreement between the numerical and the experimental results, although they correspond to two different values of G.

On the other hand, the assertion that, to a very good approximation, P is the unique relevant parameter for the dependence of α on V and λ ceases certainly to be valid for V values just above V_c, i.e., when μ is close to 1. The theory shows that the value of α at the threshold (α_c) is zero for a purely capillary anisotropy. In the presence of a kinetic anisotropy [15], α_c is a constant that does not scale as $\lambda_c V_c$, where λ_c is the critical wavelength of the cellular instability [5] (note that, in our experiments, $\lambda_c \approx 101\ \mu$m and $V_c \approx 2.8\ \mu$m s^{-1}, so that the corresponding Péclet number is ≈ 0.6). Thus, for V very close to V_c, α, as well as other morphological variables, depends not only on P, but also on μ. Experimentally, we indeed noted that, when μ is close to 1, the α data points no longer superimpose in the α versus P representation. This sensitivity of α to the temperature gradient close to V_c also clearly appears in our numerical calculations for V less than $\approx 3V_{cs}$, i.e., $\mu<3$ (it is the origin of the slight discrepancy visible between the two points obtained at $P=0.6$ in Fig. 5). This shows that the shallow-cell regime, which corresponds to this low-velocity range, is precisely the regime in which the effects of G are important.

When μ tends towards infinity, i.e., when V, and thus P, indefinitely increase at fixed λ, α tends towards α_0 since the boundary conditions are becoming equivalent to these of free growth. That increasing λ at fixed V leads to the same result is more surprising, since μ remains constant and is not necessarily large. Nevertheless, we found numerically that, at constant P ($P=5$), when λ is changed by a factor of 3 (from 55.9 to 162.8 μm; μ then varies from 8 to 25), α remains remarkably constant ($\alpha=27\pm 0.4°$ for $\alpha_0=30°$).

The comparison of our results (which, we recall, are calculated for $\alpha_0=30°$) with those found numerically by Okada and Saito [16] leads to another unexpected conclusion. These authors calculated α as a function of V for a single λ value ($\lambda/l_t=0.36$) and a single value of α_0 (17°) for a system without kinetic effects, thus with a purely capillary anisotropy $\varepsilon_c=0.1$ (the material parameters were those of a Ni-Cr steel). For P ranging between 1 and 5, their points, simply rescaled by $30/17=1.76$ (Fig. 5), superimpose onto our numerical data within $\pm 1°$. At high P values, the α versus P curve calculated by Okada and Saito tends towards α_0 more rapidly than our curve calculated for $\alpha_0=30°$. On the other hand, our data point calculated for $\alpha_0=17°$ and $P=5$ falls well in the continuity of Okada and Saito's ones. In addition, these authors also found an approximately linear dependence of α with α_0 at constant P for α_0 ranging between 0 and 25° [17]. Once again, the deviations between the various sets of data calculated for different values of α_0 can be apparently explained by the slight dependence of the shape of the α versus P curve on the value of α_0. It seems thus that, at least within the large-anisotropy limit, the scaling of α with P is essentially independent of the nature of the anisotropic interfacial property (surface tension or interfacial kinetics) involved in the dendritic-selection mechanism.

To conclude, we have demonstrated the existence of a master curve for the tilt angle α of tilted dendrites as a function of the spacing Péclet number in directional solidification. This master curve is essentially insensitive to the temperature gradient and its shape is essentially due to finite-size effects within the periodic pattern. The only significant influence of the unidirectional temperature gradient on the growth pattern is thus to make it approximately periodic. It would thus be interesting to examine if, as it apparently follows from our study, tilted dendrites with the same P dependence of α would also be observed in free growth under periodic boundary conditions [18]. In this case, this would mean that the dynamics and the selection mechanism of tilted but also of axial dendrites [19] in directional solidification obey the same rules as free-growth dendrites in a channel with periodic boundary conditions [20].

ACKNOWLEDGMENTS

We gratefully acknowledge G. Faivre and A. Karma for very fruitful discussions. Thanks are also due to H. Savary and A.-M. Pougnet, of the Centre National d'Etudes des Télécommunications, France-Télécom, Bagneux, France, for providing us with zone-refined chemicals. The experiments are supported financially by the Centre National d'Etudes Spatiales, France. T.I. benefitted from a grant of the Ministère des Affaires Etrangères, France.

[1] For a review on dendritic growth, see, for example, J. S. Langer, in *Chance and Matter*, edited by J. Souletie, J. Vannimenus and R. Stora (Elsevier, Amsterdam, 1987); D. A. Kessler, J. Koplik, and H. Levine, Adv. Phys. **37**, 255 (1988); H. Müller-Krumbhaar and W. Kurz, *Phase Transformation in Materials*, edited by P. Haasen (VCH-Verlag, Weinheim, 1991); Y. Pomeau and M. Ben Amar, in *Solids Far from Equilibrium*, edited by C. Godrèche (Cambridge University Press, Cambridge, England, 1992).

[2] E. A. Brener and V. I. Mel'nikov, Adv. Phys. **40**, 53 (1991).

[3] J. C. LaCombe, M. B. Koss, V. E. Fradkov, and M. E. Glicksman, Phys. Rev. E **52**, 2778 (1995). U. Bisang and J. H. Bilgram, Phys. Rev. Lett. **75**, 3898 (1995).

[4] S. Akamatsu, G. Faivre, and T. Ihle, Phys. Rev. E **51**, 4751 (1995).

[5] W. W. Mullins and R. F. Sekerka, J. Appl. Phys. **35**, 444 (1964).

[6] R. Trivedi, V. Seetharaman, and M. A. Eshelman, Metall. Trans. A **22**, 585 (1991).
[7] P. Oswald, M. Moulin, P. Metz, J. C. Géminard, P. Sotta, and L. Sallen, J. Phys. III **3**, 1891 (1993).
[8] J. Mergy, G. Faivre, C. Guthmann, and R. Mellet, J. Cryst. Growth **134**, 353 (1993).
[9] S. Akamatsu and G. Faivre, J. Phys. I **6**, 503 (1996).
[10] V. G. Smith, W. A. Tiller, and J. W. Rutter, Can. J. Phys. **33**, 723 (1955).
[11] Another, reliable method of controlling α_0 would be to use a rotable solidification stage. However, in the setup described in Ref. [7], only square samples of relatively small lateral dimension (about 1 cm in Ref. [7]) can be used. Our experiments require much longer samples (7 cm).
[12] T. Ihle (unpublished).
[13] A. Classen, C. Misbah, H. Müller-Krumbhaar, and Y. Saito, Phys. Rev. A **43**, 6920 (1991).
[14] This value of β_0 represents an upper bound for the average kinetic coefficient, knowing that the recoil of the front along the temperature gradient due to kinetic effects is not observable experimentally. As the shape of the α vs P master curve is essentially independent of β_0, the determination of its precise value is not central for the present purpose. It is only worth noting that the relatively high value of the ratio $D\beta_0/\Delta T_0 d_0 = 18.75$ signals that we are well in the kinetic regime.
[15] S. R. Corriell and R. F. Sekerka, J. Cryst. Growth **34**, 157 (1976).
[16] T. Okada and Y. Saito, Phys. Rev. E **54**, 650 (1996).
[17] The two systems exhibit noticeable differences in their behaviors only for α_0 values close to 45°. In the purely capillary case, the dendrites become unstable at high α_0 values. The pattern transforms into the ''seaweed'' pattern when α_0 approaches 45°. Thus, as we claimed previously (see Ref. [4]), only the anisotropy of the kinetic coefficient is able to stabilize dendrites tilted at angles higher than 40°.
[18] A closely related situation has been investigated in a recent article by R. Kupferman and D. H. Kessler [Phys. Rev. E **51**, R20 (1995)]. However, they imposed α to be equal to α_0. Accordingly, they found stable tilted arrays of dendrites only for Péclet numbers higher than about 10 (their definition of P is equal to 1/4 times ours), which is compatible with our results.
[19] Y. Saito, C. Misbah, and H. Müller-Krumbhaar, Phys. Rev. Lett. **63**, 2377 (1989).
[20] R. Kupferman, D. A. Kessler, and E. Ben-Jacob, Physica A **213**, 451 (1995).